Calculation of Electron Paramagnetic Resonance Spectra from Brownian Dynamics Trajectories: Application to Nitroxide Side Chains in Proteins

Heinz-Jürgen Steinhoff* and Wayne L. Hubbell#
*Lehrstuhl für Biophysik, Ruhr-Universität Bochum, 44780 Bochum, Germany and #Jules Stein Eye Institute and Department of Chemistry and Biochemistry, University of California, Los Angeles, California 90024-7008

ABSTRACT We present a method to simulate electron paramagnetic resonance spectra of spin-labeled proteins that explicitly includes the protein structure in the vicinity of the attached spin label. The method is applied to a spin-labeled polyleucine α-helix trimer. From short (6 ns) stochastic dynamics simulations of this trimer, an effective potential energy function is calculated. Interaction with secondary and tertiary structures determine the reorientational motion of the spin label side chains. After reduction to a single particle problem, long stochastic dynamic trajectories (700 ns) of the spin label side-chain reorientation are calculated from which the Lamor frequency trajectory and subsequently the electron paramagnetic resonance spectrum is determined. The simulated spectra agree well with experimental electron paramagnetic resonance spectra of bacteriorhodopsin mutants with spin labels in similar secondary and tertiary environments as in the polyleucine.

INTRODUCTION

Electron paramagnetic resonance spectroscopy (EPR) of spin-labeled biomolecules has been a highly successful technique that provides insight into the structure and the dynamics of proteins and nucleic acids (Berliner, 1976, 1979, 1989). Site-directed mutagenesis has allowed the introduction of spin-labeled side chains at any desired site in a protein using cysteine substitution mutants (see Hubbell and Altenbach, 1994, for a review). One of the most powerful approaches to obtain structural information from the labeled protein is the analysis of the collision rates of the attached spin labels with hydrophobic and hydrophilic Heisenberg exchange reagents (Altenbach et al., 1990, 1994a; Hubbell and Altenbach, 1994). This technique allows determination of the topography of the polypeptide chain with respect to the membrane/solution interface, and the identity and orientation of secondary structure in selected regions. Moreover, recent studies of a number of spin-labeled bacteriorhodopsin mutants has provided evidence that the continuous wave (CW) EPR spectral line shape contains direct information about the tertiary structure of the protein in the vicinity of the nitroxide side chain (Altenbach et al., 1994b). To better understand the nitroxide side-chain motion, the EPR spectral line shape and its dependence on the local tertiary structure, we have developed tools that allow continuous wave EPR spectra of spin-labeled molecules to be simulated with consideration of the spin label binding site structure on an atomic level. The methodology and first results are presented in this paper.

The EPR spectral line shape is determined by the molecular reorientational dynamics of the attached spin label and its constraints over correlation times ranging from 10^{-11} to 10^{-6} s. According to the Kubo-Tomita theory, it is possible to simulate EPR spectra on the basis of different dynamic models (Freed, 1976; Schneider and Freed, 1989). EPR spectra of solvated spin labels that undergo Brownian reorientational diffusion, jump diffusion, or free diffusion have been simulated. These simulations show excellent agreement with the corresponding experimental data (Freed, 1976). Anisotropies of the reorientational motion of anisotropic molecules, e.g., spin-labeled lipids, were accounted for by introducing simple potentials (Ge and Freed, 1993). If, however, spin labels are bound to a protein, the potential surface that determines its motion can be extremely complex, involving interactions with the protein backbone, the adjacent side chains, and collisions with solvent molecules. In addition, spatial restrictions of the spin label side-chain motion influence an EPR spectrum in a similar way as an increase of the reorientation correlation time due to differences in local friction. A unique extraction of both of these parameters from the experimental spectrum on the basis of dynamic models seems to be impossible. Therefore, an alternative technique based on molecular dynamics (MD) simulations of the spin-labeled protein molecule is explored. Molecular dynamics or stochastic dynamics (SD) simulations offer the advantage to study the influences of the structure of the spin label binding site on the EPR spectral line shape with atomic resolution. In another report, EPR spectroscopy and MD simulations were combined to study the dynamics of nitroxide side chains in the picosecond time range (Steinhoff and Karim, 1993). Robinson et al. (1992) have shown that CW-EPR line shapes can be simulated directly by using trajectories generated by classical Brownian dynamics simulations in the nanosecond time range. We have combined and extended both methods and

Received for publication 19 April 1996 and in final form 18 June 1996.
Address reprint requests to Dr. Heinz-Jürgen Steinhoff, Lehrstuhl für Biophysik, Ruhr-Universität Bochum, 44780 Bochum, Germany. Tel.: 49-234-7004463; Fax: 49-234-7094238 E-mail: steinhbt@rz.ruhr-uni-bochum.de.

0006-3495/96/10/2201/12 $2.00

present simulated EPR spectra of spin labels with different tertiary interactions in a trimer of polyleucine helices.

THEORY

Methods overview

First, we give an overview of the computational technique that is used to generate information about the motional properties of spin labels bound to proteins and the calculation of the EPR spectra thereof. The orientation trajectory of a spin label, which is bound to a macromolecule, contains all the information needed to calculate the CW-EPR spectrum. However, for the simulation of a proper EPR spectrum, the length of the trajectory has to be of the order of the transversal relaxation time, T_2, i.e., of the order of several 100 ns. Modern computers allow dynamic simulations of macromolecules with solvent included only up to several hundred picoseconds (Brooks, 1995). For small molecules, however, trajectories in the ns time range can be simulated. Therefore, an alternative approach is used here. The influence of the neighbor side chains, the backbone atoms, and the solvent on the single nitroxide side chain is considered in two succeeding steps. The effect of the neighbor side chain and of the backbone on the space accessible for the orientation of the nitroxide is approximated by a potential of mean force, i.e., a potential that includes the average interaction of the nitroxide with these neighbor atoms. It is derived from a molecular dynamics or stochastic dynamics simulation of the entire spin-labeled polypeptide with fixed backbone atoms. The MD simulation is performed at high temperature to overcome small potential barriers attributable to van der Waals attractive forces. This guarantees that the total space accessible for the reorientation of the nitroxides is covered within a reasonable computation time. Once the average effective potential is calculated, the nitroxide is approximated by a single particle exposed to a mean force, which results from this potential. The deviation of the real force from the mean force caused by the solvent and fluctuating side chains is then represented by a random fluctuating force. For this purpose the Langevin equation for rotational motion is solved numerically, which yields the orientation trajectory $\Omega(t)$ of the nitroxide spin label with trajectory lengths in the microsecond time range. The Lamor frequency and the magnetization trajectories are then calculated from $\Omega(t)$. The EPR absorption spectrum is then given by the Fourier transform of the magnetization trajectory.

The Langevin equation

The EPR spectral line shape of a single nitroxide spin label is completely determined by the reorientational behavior of the nitroxide group. The simplest form of the stochastic rotational dynamics of a single particle is represented by the Langevin equation (Wolynes and Deutch, 1977)

$$I_i \frac{d\omega_i(t)}{dt} = -I_i f \omega_i(t) + T_i(\Omega(t)) + R_i(t) \qquad (1)$$

Here, $\omega_i(t)$ are the x, y, or z components of the angular velocity of the particle having the moment of inertia I_i. For simplicity the friction coefficient f in the damping term is assumed to be independent of position and time. $T_i(\Omega(t))$ is the systematic torque for orientation $\Omega(t)$. $T_i(\Omega(t))$ is given by the derivative of the potential of the mean force with respect to the rotation angle around axis i, ϕ_i,

$$T_i(\Omega) = -\frac{dU_{eff}(\Omega)}{d\phi_i} \qquad (2)$$

The random part in Eq. 1, R_i, is described by a Gaussian distribution with zero mean and satisfies the fluctuation dissipation relation

$$\langle R_i(0) R_j(t) \rangle = 2 I_i kT f \delta_{ij} \delta(t) \qquad (3)$$

where δ is a Dirac delta function and kT is the product of the Boltzmann constant and temperature. The friction coefficient f is related to the rotational diffusion coefficients D_i by the Einstein equation

$$D_i = \frac{kT}{I_i f} \qquad (4)$$

Assuming the systematic force to be constant during Δt and assuming that $1/f \ll \Delta t$, one obtains the algorithm for the reorientation around axis i at time $n * \Delta t$, $\phi_{n,i}$, (van Gunsteren, 1981)

$$\begin{aligned} \phi_{n+1,i} &= \phi_{n,i} + (kT)^{-1} D_i T_{n,i} \Delta t + \Phi_{n,i} \\ \langle \phi_{n,i} \rangle &= 0 \\ \langle \phi^2_{n,i} \rangle &= 2 D_i \Delta t \end{aligned} \qquad (5)$$

This algorithm, which applies to the diffusive regime where the distribution of the velocity relaxes much more rapidly than that of the position, is used here. The $\Phi_{n,i}$ values were calculated by using a normally distributed random number generator similar to the subroutine GAUSS of the GROMOS program library (BIOMOS, Groningen, the Netherlands). Eqs. 1–5 represent the simplest form of stochastic dynamics, called diffusive Brownian dynamics, because neither spatial nor time correlations are taken into account (van Gunsteren et al., 1981).

The effective potential energy function

The effective potential energy function $U_{eff}(\Omega(t))$, Eq. 2, is required to determine the torques in the Langevin equation. This function is given by the free energy that can be estimated from molecular dynamics or stochastic dynamics trajectories of the spin labeled polypeptide. The orientation population of the nitroxide in the polypeptide-fixed reference frame is evaluated from the trajectory in the angle interval $(\alpha, \alpha + d\alpha; \beta, \beta + d\beta; \gamma, \gamma + d\gamma)$ as a function of the three Euler angles $\Omega = (\alpha, \beta, \gamma)$. This orientation population is identified with $W(\alpha, \beta, \gamma) d\alpha\, d\beta\, d\gamma$, where W

is a probability density function. The free energy is then given by

$$U_{\text{eff}}(\Omega) = -kT \ln W(\Omega) + C \tag{6}$$

and is calculated from 6° intervals of α, β, and γ. C is an arbitrary constant. To avoid artifacts due to the discrete and noisy character of the free energy surface, a function $W'(\Omega)$ is fitted to the angle population density surface $W(\Omega)$

$$W'(\Omega) = \sum_{\text{h}} a_{\text{h}} e^{\left(\frac{(\alpha_{\text{h},0}-\alpha_{\text{h}})^2}{2\sigma_{\alpha\text{h}}} + \frac{(\beta_{\text{h},0}-\beta_{\text{h}})^2}{2\sigma_{\beta\text{h}}} + \frac{(\gamma_{\text{h},0}-\gamma_{\text{h}})^2}{2\sigma_{\gamma\text{h}}}\right)} \tag{7}$$

The subscript 0 denotes the center angles of potential extremes with widths σ, h is the number of these extremes. The torques are then derived from Eq. 2 using the probability density given by Eq. 7.

EPR spectra simulations from Brownian dynamics trajectories

The magnetic moment

The simulations of EPR spectra from Brownian dynamics trajectories of the spin label motion are based on a simple, classical treatment of the motion of the magnetic moment M of a given spin packet with Lamor frequency ω. Assuming that no forces other than an applied magnetic field B_0, which defines the laboratory z-direction, acts on the spins, the equation of motion of M is of the form

$$\frac{dM}{dt} = \gamma M \times B_0 \tag{8}$$

where γ represents the magnetogyric ratio of the spins under consideration. In magnetic resonance spectroscopy the magnetization is detected in the x, y plane. The solution of the equation of motion for the components of M in this plane is

$$M_+(t + \Delta t) = M_+(t)\exp(-2\pi i \nu \Delta t) \tag{9}$$

where the complex magnetization vector M_+ is given by $M_x + iM_y$, and $2\pi\nu$ is the fundamental Lamor frequency, γB_0. This is given by the eigenvalues of the spin Hamiltonian of the considered spin-bearing molecules. Because of anisotropies of the g and hyperfine tensors, the Hamiltonian, and therefore the Lamor frequency, depends on the orientation Ω of the considered molecule with respect to the magnetic field. To obtain the magnetization trajectory for an entire sample of paramagnetic molecules, $M_+(\Omega, t)$ has to be averaged over all possible initial orientations of Ω, Ω_0, with the proper equilibrium distribution $P_0(\Omega_0)$,

$$\langle M_+(t)\rangle = \int P_0(\Omega) M_+(\Omega, t) d\Omega_0 \tag{10}$$

The observed dispersion and absorption CW-EPR signals are then found as the real and imaginary part of the Fourier transform of $\langle M_+(t)\rangle$.

The Hamiltonian

The orientation-dependent Lamor frequency is calculated from the eigenvalues of the spin Hamiltonian. A proper spin Hamiltonian that describes the behavior of a collection of nitroxide spin labels is

$$H = H_{\text{Zeeman}} + H_{\text{hyperfine}} \tag{11}$$

$$= \beta_e S \mathbf{g} B_0 + S \mathbf{A} I \tag{12}$$

Here, we assume that the local spin concentration is low, that we may neglect all terms of electron-electron interaction. β_e is the electron Bohr magneton, S and I are the electron and nuclear spin operators, respectively. The g-factor tensor $\mathbf{g}$ and the hyperfine tensor $\mathbf{A}$ are diagonal in the nitroxide coordinate system xyz, with the principle values g_{xx}, g_{yy}, g_{zz} and A_{xx}, A_{yy}, and A_{zz}. The x axis of the nitroxide coordinate system is defined by the direction of the N-O bond, the z axis is parallel to the nitrogen and oxygen $2p$ orbital, and y is perpendicular to x and z.

It is reasonable to have the spin operators and therefore H expressed in the laboratory coordinate system X, Y, Z, where Z is defined to be the direction of the laboratory magnetic field B_0. The spin Hamiltonian then takes the form

$$H = \beta_e S L \mathbf{g} L^\tau B_0 + S L \mathbf{A} L^\tau I \tag{13}$$

where L is the transformation matrix, which rotates the nitroxide x, y, z axes into the laboratory X, Y, Z axes, and τ denotes transpose. There are several convenient approximations of Eq. 13 that allow calculation of the eigenvalues of H and that have been shown to give good fits to experimental data for nitroxide radicals. The high field approximation assumes the hyperfine field to be much less than the laboratory field, and S and I are quantized along the laboratory z axis. In this approximation, the terms containing x and y components of S and I are neglected. The solution of the eigenvalue problem yields the transition energies and therefore resonance frequencies, which are given by

$$h\nu_{\text{Ms,Mi}} = g_{ZZ}\beta_e B_0 M_S + A_{ZZ} M_S M_I \tag{14}$$

with the spin quantum numbers $M_S = \pm 1/2$ and $M_I = -1$, 0, $+1$. The terms g_{ZZ} and A_{ZZ} are related to the principle values of the tensors $\mathbf{g}$ and $\mathbf{A}$ by

$$g_{ZZ} = g_{xx} l_{Zx}^2 + g_{yy} l_{Zy}^2 + g_{zz} l_{Zz}^2 \tag{15}$$

$$A_{ZZ} = A_{xx} l_{Zx}^2 + A_{yy} l_{Zy}^2 + A_{zz} l_{Zz}^2$$

The matrix elements of L, l_{ij}, are the direction cosines between the nitroxide and the laboratory axes. For axial symmetry of $\mathbf{A}$ we can simplify $A_{xx} = A_{yy} = A_\perp$, and $A_{zz} = A_\parallel$, and obtain

$$A_{ZZ} = a - \Delta A(1 - 3\cos^2\beta) \tag{16}$$

with

$$a = \frac{1}{3}(2A_\perp + A_\parallel)$$
$$\Delta A = \frac{1}{3}(A_\parallel - A_\perp) \quad (17)$$

where β is the angle between the molecular z axis and the external magnetic field. This high field limit approximation gives rigid limit splittings that are considerably smaller than the splittings calculated from the exact solution by more than 4 G (Libertini and Griffith, 1970) at X-band frequency. This discrepancy becomes less important for high frequency EPR (Q-band and higher) and is unimportant for model calculations (Robinson et al., 1992). However, we aim at quantitative comparison of simulated and experimental spectra in the X-band. Therefore, a second-order approximation is used that will be discussed below. First, however, we look at an unambiguous advantage of the high field approximation, Eq. 14, and this is its behavior when the influence of fast reorientational motion on the Hamiltonian is considered. Our method implies that the Lamor frequencies, i.e., the eigenvalues of the Hamiltonian, are spatially averaged within a certain time interval. If the average change in molecular orientation during the characteristic time $h/(A_\parallel - A_\perp)$ becomes larger than 1 rad, the resulting spectral splitting is in general given by the eigenvalues of a time-averaged Hamiltonian calculated from Eq. 13 (Van et al., 1978). It can be demonstrated that the eigenvalues of this time-averaged Hamiltonian equal the spatial-averaged eigenvalues calculated from Eq. 14. For example, because the complete spatial averaging of $(1 - 3\cos^2\beta)$ in Eq. 16 yields zero, the solution of Eq. 14 gives the well-known fast motional limit result of three lines centered at a B-field value given by the isotropic g value, 1/3 trace **g**, and separated by the isotropic hyperfine splitting a, 1/3 trace **A**. Our simulations for isotropic Brownian rotational diffusion show good agreement with exact spectra calculated by Freed's program (Freed, 1976) for correlation times $\tau < 5$ ns. Thus, the high field treatment is an appropriate approximation for the fast motional region.

However, an approximation, which yields considerably more accurate splittings in the slow motional region ($\tau \geq 5$ ns), is obtained by including the pseudosecular terms $S_Z I_X$ and $S_Z I_Y$ (intermediate field treatment). In the absence of motion, the transition energies are then given by (Libertini and Griffith, 1970)

$$h\nu_{Ms,Mi} = g_{ZZ}\beta_e B_0 M_S + (A_\Delta^2 + A_{ZZ}^2)^{1/2} M_S M_I \quad (18)$$

with

$$A_\Delta = -3\,\Delta A \sin\beta\cos\beta \quad (19)$$

This solution has been shown to give very good fits to accurate experimental powder spectra or single crystal data (Libertini and Griffith, 1970; Steinhoff, 1988). However, spatial averaging of the eigenvalues, Eq. 18, does not lead to the correct splitting in the fast motional limit, as can immediately be realized from the nonlinear dependence of $h\nu$ on **A**. To account for the time averaging of the pseudosecular terms in the Hamiltonian due to reorientational motion we introduce the correlation function $g_\beta(\tau) = \langle\cos\beta(t)\cos\beta(t+\tau)\rangle$ of the angle β, which is determined from the respective reorientation trajectory of the nitroxide label. The term A_Δ in Eq. 18 is multiplied by the normalized correlation function at time $h/\Delta A$, $g_\beta(h/\Delta A)/g_\beta(0)$. An increase of the mobility of the label from the rigid limit to the fast motional limit changes this function from 1 to 0, and Eq. 18 reduces to Eq. 14. This approach covers the whole motional correlation time region of interest with high accuracy, as will be demonstrated in the next section.

Eq. 18 is written in terms of one matrix L that rotates the nitroxide x, y, z axes into the laboratory X, Y, Z axes. We introduce one additional intermediate coordinate system X',Y', Z', the peptide or sample system, which we define by the time average of the nitroxide molecular axes directions x, y, z. The transformation matrices L' and L'', which are defined in terms of the three Euler angles α, β, γ, rotate the nitroxide coordinate system x, y, z into the sample system X', Y', Z', and afterward into the laboratory coordinate system X, Y, Z:

$$\begin{pmatrix} X \\ Y \\ Z \end{pmatrix} = L' \begin{pmatrix} X' \\ Y' \\ Z' \end{pmatrix} = L'L'' \begin{pmatrix} x \\ y \\ z \end{pmatrix} \quad (20)$$

In the absence of motion or for isotropic motion the nitroxide system x, y, z and the peptide system X', Y', Z' are identical. The matrix elements l_{ij} in Eq. 15 have to be replaced by the matrix elements of L', l'_{ij}, and the transition frequencies are then given by Eq. 18. The CW-spectrum is obtained by applying Eqs. 9 and 10 followed by a Fourier transformation.

In the presence of residual motion of the spin label with respect to the protein, the matrix L'' is time dependent. For calculation of the transition frequencies, the l_{ij} in Eq. 15 have to be replaced by the respective elements of the matrix products of the L' and L'' matrices. Application of Eq. 18 for every time step of the orientation trajectory yields the Lamor frequency trajectory, $\nu(t)$. If the time interval Δt of the orientation trajectory is chosen so small that

$$\nu(t + \Delta t) \approx \nu(t) \quad (21)$$

then Eq. 9 can be regarded as a valid approximation that is used to calculate the magnetization trajectory. For an isotropic orientation distribution of the protein molecules, $P(\Omega)$ is given by the sine of the angle between Z and Z'.

Molecular dynamics simulations of a spin-labeled polyleucine trimer

A central goal of our approach is the physical understanding of the influence of protein local structure on the EPR

spectrum, which reflects the residual dynamics of the spin label and the dynamics of the local environment. The α-helix is the most common type of secondary structure found in proteins, and approximately parallel arrangements of α-helices are frequently found in membrane proteins. In our study, a molecular dynamics simulation is carried out for three different positions of a spin label in a trimer of polyleucine α-helices. The simulations provide insight into the structurally determined restrictions to nitroxide side-chain orientation, and also allow for the determination of the free energy surface of a SD-EPR spectral calculation. The results indicate that tertiary interactions of the nitroxide side chains with neighboring helices strongly influence the EPR spectral lineshapes.

The molecular model

A polyleucine (L_{11}) trimer was constructed using Prosimulate (BIOSTRUCTURE, Illkirch, France) and the GROMOS program library (BIOMOS). The three α-helices are arranged as shown in Fig. 1. Each of the monomers is modified by replacement of the central leucine with a nitroxide side chain. The most commonly used nitroxide side chain is introduced by reaction of cysteine with the spin label (1-oxyl-2,2,5,5 tetramethylpyrroline-3-methyl) methanethiosulfonate, and is designated R1 (Fig. 2). The spectra of this disulfide-linked side chain have been found to be very sensitive to the local protein structure and structural changes during the function of the protein (Altenbach et al., 1990; Miick et al., 1991; Steinhoff et al., 1994). The α-helices are rotated around their axes to expose the three spin label side chains to tertiary interaction of different extent (Fig. 1). The nitroxide of spin label 1 is expected to be only slightly influenced in its reorientational motion by the interaction with neighboring helix atoms. In contrast, the C_α-C_β bond direction of spin label side chain 2 is oriented further toward the neighboring helix backbone providing a position of the sulfurs to interact more efficiently with the neighboring tertiary structure. Thus, the interaction of spin label side-chain atoms with atoms of the adjacent helix during reorientation is more likely for spin label 2 than for spin label 1. The reorientational motion of spin label 3 is expected to be even much more restricted because of possible interactions with backbone and side-chain atoms of the two adjacent helices.

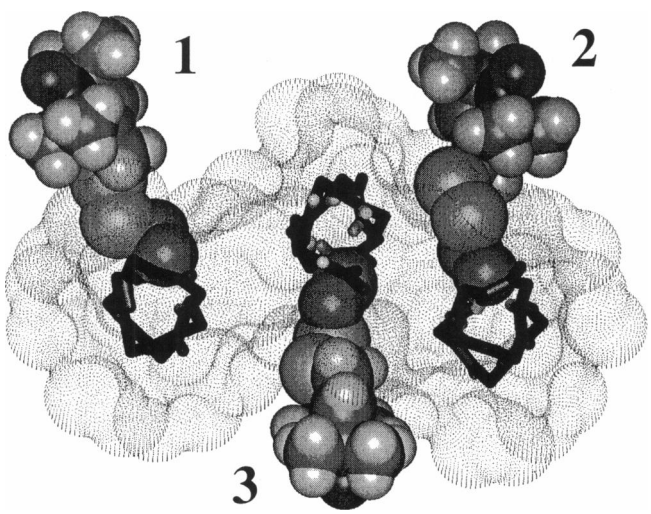

FIGURE 1 View of the spin-labeled polyleucine trimer along the helices axes. The backbone bonds are shown as sticks and the atoms of the three spin label side chains are shown space filled. The dotted lines display the projection of the polypeptide surface.

Reorientation trajectories for the nitroxides were calculated from stochastic dynamics simulations by means of the GROMOS program library. Aliphatic CH, CH2, and CH3 groups, as well as aromatic CH groups were treated as extended carbon atoms. The total number of atoms in the molecule was 279. Bond lengths and the positions of the backbone atoms were constrained using the SHAKE (van Gunsteren et al., 1982) algorithm with relative accuracy of 10^{-4}. The nitroxide side chain is neutral, i.e., influences of charges on the residual motion are not expected. Coulomb interactions were therefore excluded from the calculations to save computation time. After energy minimization, the backbone atoms were fixed and the system was first equilibrated at 50 K, then heated up to 300 K and finally to 600 K. Using a friction coefficient of 4 ps^{-1}, the time step of the integration of the classical equations of motion were set to 4 fs (van Gunsteren et al., 1982). Trajectories with lengths of 6 ns were calculated for 300 and 600 K. The computation was performed using an IRIS 4D35 (Silicon Graphics, Mountain View, California), the total computation time was 520 h.

To separate the influences of tertiary interaction on the spin label side-chain motion from the reorientational restrictions due to torsion barriers, additional stochastic dynamic simulations were performed with a spin label attached to a single fixed cysteine and for an unbound, freely diffusing nitroxide ring. The trajectory length of each of these simulations is 1.2 ns.

To quantitatively describe the orientation fluctuation of the nitroxide side chain, the orientation history of the z axis of the nitroxide ring is calculated from the cross-product of the unit vectors in the C_2 to N and the C_5 to N directions. The deviation of the orientation of z' from the initial orientation of the nitroxide plane, z, is expressed in terms of Euler angles, α, β, and γ, which are used to display the orientation trajectory.

RESULTS

Stochastic dynamics simulations

Freely diffusing nitroxide ring

The correlation function $g(\tau)$ of the Euler angle β for the spin label diffusing freely in solution at 300 K reveals an exponential decay with a correlation time of 6 ps and $g(\tau = 0) = 0.33$. The normalized behavior of $g(\tau)$ is shown in Fig.

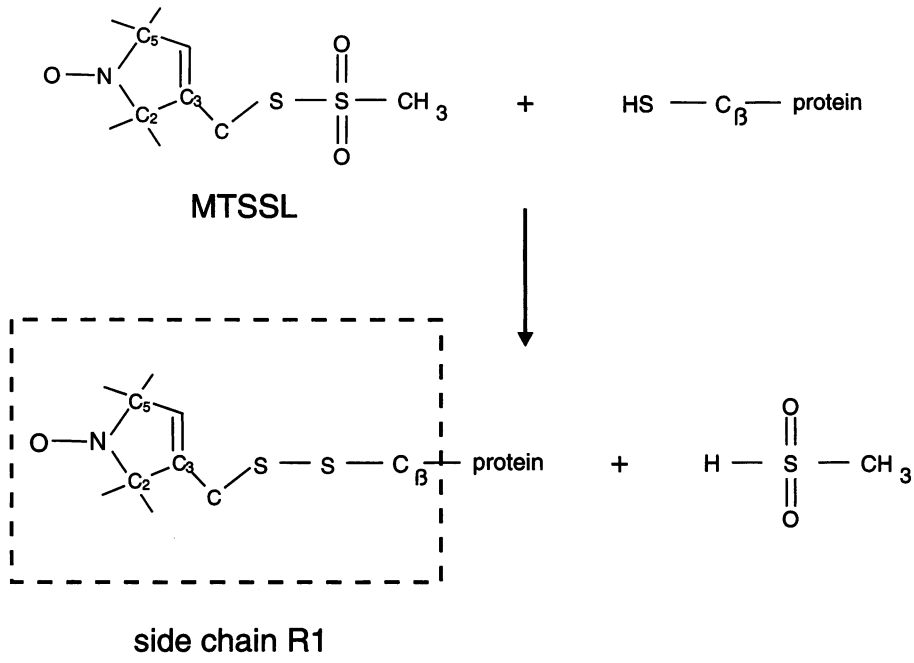

FIGURE 2 Structure of the spin label (1-oxyl-2,2,5,5 tetramethylpyrroline-3-methyl) methanethiosulfonate (MTSSL) and its reaction with a protein to yield the spin label side chain R1.

3. This behavior is expected for a particle that undergoes isotropic reorientational motion in a viscous medium. From experimental studies the rotational correlation time of a nitroxide ring, which diffuses freely in aqueous solution at 295 K, is determined to be 17 ps (Jolicoeur and Friedman, 1971). Thus, the value for the friction coefficient f chosen for the simulations yields a viscosity in the spin label environment that amounts to one-third of the viscosity of water. This value of f allows to get representative data within reasonable computation time, and the resulting value of the environmental viscosity is close enough to that of water to allow comparisons of the simulations with experiments.

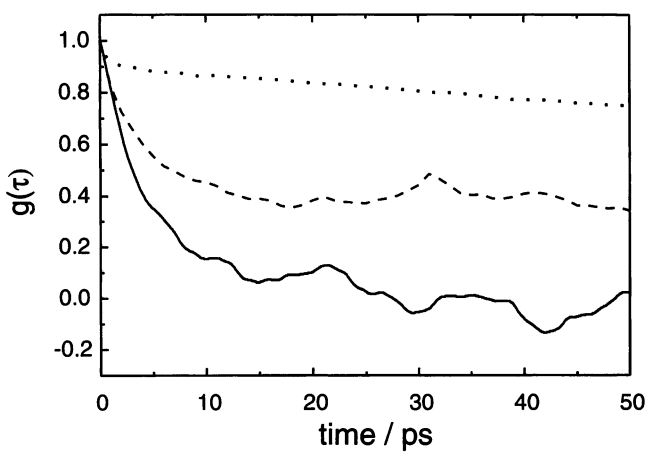

FIGURE 3 Correlation function for the reorientation of the nitroxide z axis determined from stochastic dynamics simulations at 300 K for three different spin label environments. Full line, nitroxide ring diffusing freely in solution; broken line, spin label side chain R1 attached to a space-fixed cysteine amino acid; dotted line, spin label side chain R1 attached to an α-helix (spin label 1 of the trimer shown in Fig. 1).

Motion of spin labels attached to a single cysteine or to an α-helix at 300 K

To study the effects of the covalent binding on the reorientational motion of the nitroxide ring, the spin label is attached to a single cysteine amino acid, whose back bone atoms are fixed in space. The reorientational motion of the spin label side chain is now subject to torsional barriers that prevent isotropic reorientation. This is seen from the correlation function that exhibits biphasic behavior (cf. Fig. 3). After a fast decay with a correlation time comparable to the freely diffusing case, a second much slower decay is visible. The correlation time of this phase is of the order of 100 ps.

The next step is to enlarge the molecular segment to which the spin label is attached. For that purpose consider spin label 1 that is attached to the sulfhydryl-group of the cysteine in the polyleucine trimer (cf. Fig. 1). Attractive and repulsive forces due to van der Waals interaction of the nitroxide ring with the secondary structure determine the reorientational motion of the spin label. The inspection of the reorientation trajectory (Fig. 4 *a*) reveals that the nitroxide motion consists of fast reorientational oscillations within local potential minima and rare jumps between these discrete potential traps. Three potential minima can be separated by their different mean angles β. These potential valleys are characterized by the orientation of the ring with respect to the α-helix to maximize the number of van der Waals contacts. The correlation time of the fast oscillation is in the order of the value of τ of the freely diffusing nitroxide ring. The amplitude of this fast reorientational

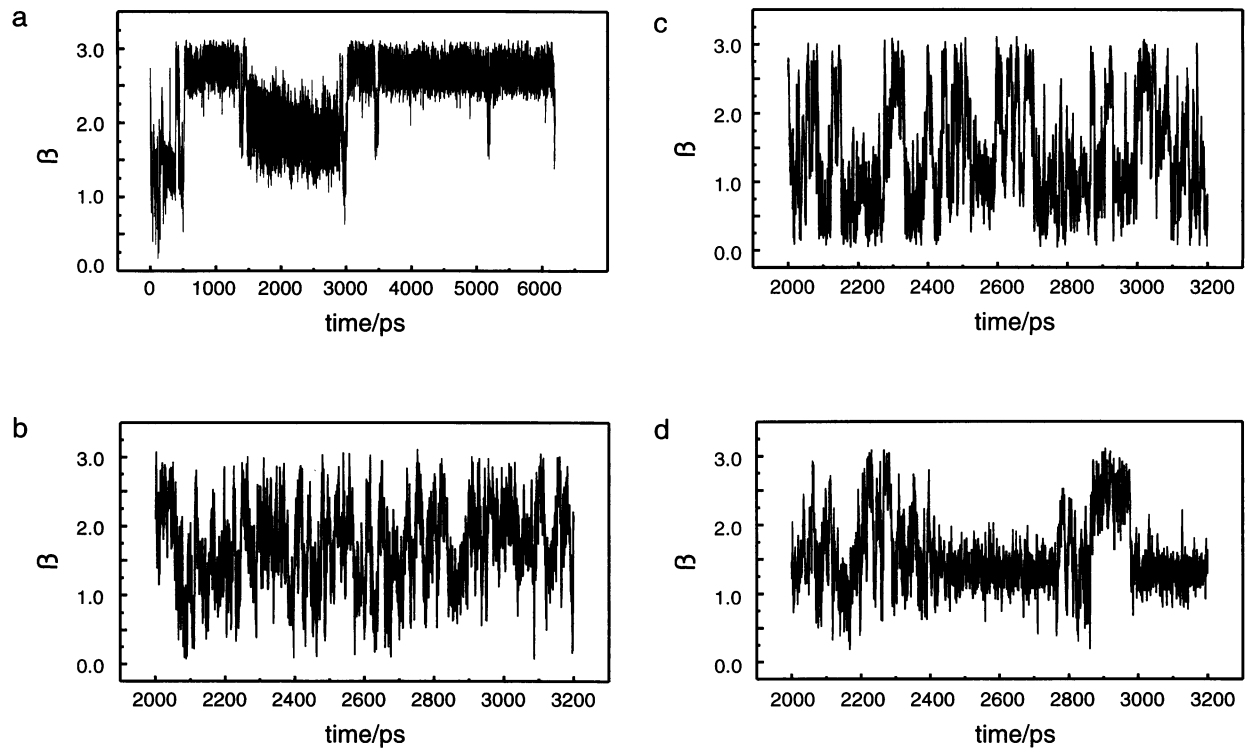

FIGURE 4 The reorientational motion of the nitroxide z axis with respect to a space-fixed axis. (*a*) The whole trajectory for spin label side chain 1 determined for 300 K is shown. Parts of the 6-ns trajectories of the trimer determined for 600 K are shown for: (*b*) spin label side chain 1; (*c*) spin label side chain 2; and (*d*) spin label side chain 3.

oscillation is different for the different potential valleys. The trajectory segment between 1.5 and 3 ns is characterized by an average value of β of 1.8 rad and an oscillation amplitude of ± 0.4 rad (23°). For the trajectory segment between 3.5 and 5.0 ns we estimate an average value of β of 2.7 rad and an amplitude of oscillation of ± 0.25 rad (14°). The correlation time of the rare jumps between these states is found from the correlation function to exceed 500 ps (cf. Fig. 3). The reorientational motion of spin labels 2 and 3 attached to the polyleucine trimer is more restricted (not shown). The trajectories mainly display oscillational behavior within local minima, only three jumps between these minima are visible for label 2. No reorientations of large amplitudes are detected for label 3 within the simulation time of 6 ns.

The determination of the free energy surface for the spin label reorientational motion from a stochastic dynamics trajectory requires the characterization of the entire angle space accessible to the nitroxide ring. To perform this task within a reasonable computation time, means have to be found to increase the transition rates of the system to pass across local potential barriers. A simple approach is to increase the system temperature that is applied in the following to the three spin labels bound to the polyleucine trimer.

Spin label motion in a polyleucine trimer at 600 K

At 600 K the potential barriers, which are due to the short range nonbonded contacts of the ring atoms with the backbone, are overcome as can be seen from the trajectory parts shown in Fig. 4, *b–d*. Parts of the orientation trajectory of the nitroxide z axes with respect to a space-fixed axes are shown for the three spin labels attached to the polyleucine trimer. Several complete rotational transitions can be observed for each of the three nitroxide rings within the time gap shown. The restriction of the reorientational motion increases from site 1 to 3. This can be deduced from the decreasing probability to find large scale transitions when comparing the spin label motion of sites 1, 2, and 3. The trajectory of site 3 clearly exhibits two different kinds of reorientational motion that we have already discussed for the 300K simulation: a fast oscillation of small amplitude within a potential valley, and transitions between different potential minima.

From the orientation trajectories of the nitroxide planes the population densities of the orientations are shown in Fig. 5. The orientation of the z axes of spin label 1 covers nearly the entire angle space with a sine β weighting similar to what is expected for an isotropic orientation distribution of a particle. The reorientational motion of spin labels 2 and 3 is more restricted as can be judged from the angle population density, which shows distinct extremes. The orientation of spin label 2 covers nearly the whole orientation space, however, the probability distribution shows two maxima at $\alpha = \beta = 1$ rad and $\alpha = -1$, $\beta = 1.5$ rad. Spin label 3 occupies mainly two different orientations, and large parts of the angle space are totally excluded. These two main

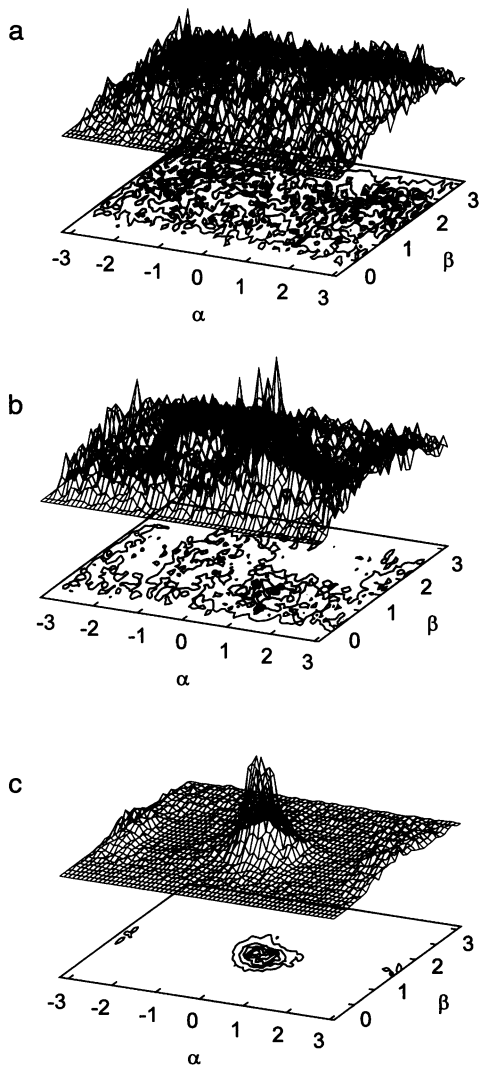

FIGURE 5 Angle population densities as a function of two of the three Euler angles, α and β, calculated from the whole lengths of the trajectories for (*a*) spin label side chain 1; (*b*) spin label side chain 2; and (*c*) spin label side chain 3.

density maxima refer to the two orientations of the nitroxide ring lying between the two adjacent helices with the ring plane oriented approximately parallel to the long helix axis. The reorientation between these two major orientations is performed by a jump diffusion-like process as can be seen from the trajectory part shown in Fig. 4 *d*.

To further understand the origin of the observed restriction of motion, the fluctuations of the dihedral angles of the whole spin label side chain were extracted from the stochastic dynamics history files. The values are shown in Table 1. The first three dihedral angles, starting from the nitroxide ring, show a similar behavior in all three cases. The rms deviation from the mean value for the first two dihedral angles is close to the value found for a random distribution of angles, which is 0.78. A very low fluctuation amplitude is observed for the disulfide bond dihedral angle, which is due to the high rotation potential barrier preventing

TABLE 1 Fluctuations of the spin label dihedral angles (the root mean square deviation from the mean value is given)

Spin label	$\Psi_{C3\text{-}C}$	$\Psi_{C\text{-}S}$	$\Psi_{S\text{-}S}$	$\Psi_{S\text{-}C\beta}$	$\Psi_{C\beta\text{-}C\alpha}$
1	0.77	0.80	0.29	0.66	0.66
2	0.80	0.85	0.27	0.52	0.42
3	0.86	0.69	0.28	0.26	0.61

a rotation around this bond. The S-C_β and C_β-C_α dihedral angles show intermediate flexibility for spin label 1, however, the low values of fluctuations of both of these angles reflect the strong tertiary interaction of the spin label side chains 2 and 3 with the neighboring helices. The C_β-C_α bond of spin label 2 is oriented toward the middle helix in a manner that flips around this bond are very unlikely due to the bulky disulfide group (see Fig. 1). The fluctuation amplitudes of the dihedral angles C-S and S-C_β is lowest for spin label 3. The presence of two helices on both sides of the disulfide group strongly restrict flips of these angles. Thus, the different extent of interaction of the bound spin label side chains with the tertiary structure in the spin label environment is mainly reflected in the restricted fluctuation behavior of the dihedral angles of the C-S and S-C_β bonds.

EPR spectra simulations

Isotropic reorientational motion of a nitroxide

We first calculated stochastic dynamic trajectories for a free particle with rotational diffusion coefficients D ranging from $0.3 * 10^9\ s^{-1}$ to $0.3 * 10^6\ s^{-1}$. The time interval Δt in Eq. 5 was chosen between 10 and 40 ps depending on the diffusion coefficient *D*. The trajectories were calculated for a total time of 700 ns. From these orientation trajectories the magnetization trajectories were calculated for 2^{14} steps of 40 ps each, leading to a total length of 655 ns. Before Fourier transformation was performed, the magnetization trajectory was zero filled in the time range from 655 to 1300 ns yielding a resolution of 0.25 G between points in the frequency domain. First derivative EPR simulations, each generated by 80 trajectories, are shown in Fig. 6. Each of the trajectories is rotated which leads to 64 different initial orientations and a total number of $64 * 80 = 5120$ trajectories. The initial orientation distribution is normalized to yield isotropic behavior. To account for an additional inhomogeneous line broadening the magnetization trajectories are multiplied by $\exp(-t/T_2)$, which is equivalent to convolution of the spectra with a Lorentzian in the frequency domain. This additional spectral broadening is justified by the presence of inhomogeneous broadening mechanisms due to spin-spin interaction, e.g., which might influence experimental spectra. In our calculations the additional line broadening provides spectra with good signal to noise ratio within reasonable computation time. For the spectra shown in Fig. 6 a Lorentzian broadening of 2.5 G is applied. Alternatively, the spectra may be convoluted with a Gaussian function to account for unresolved proton hyperfine interaction.

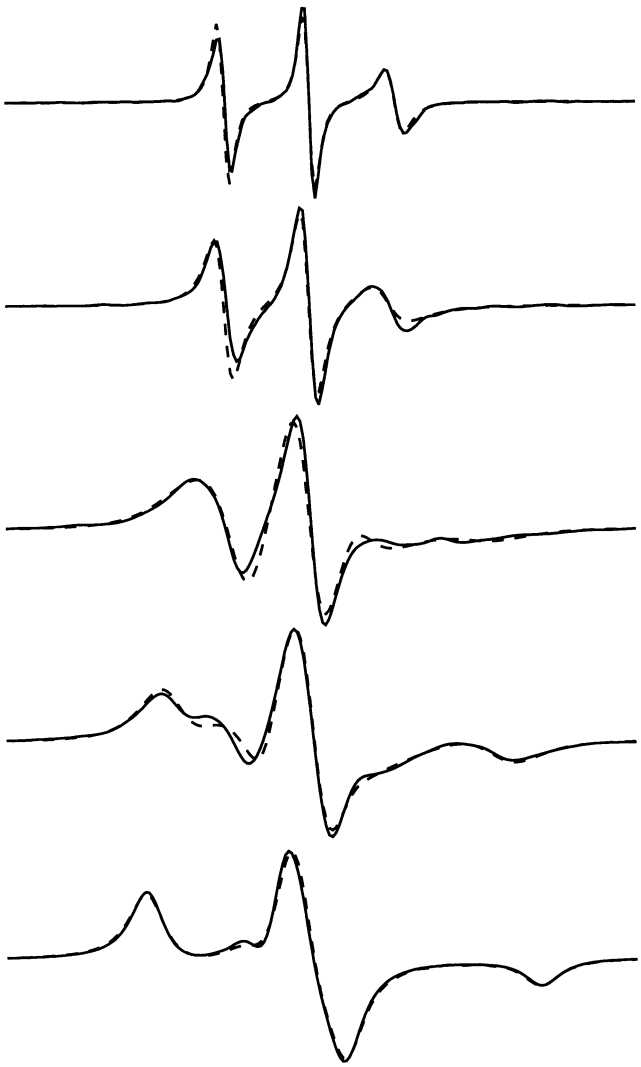

FIGURE 6 EPR spectra simulations each generated by 5120 Brownian diffusion trajectories calculated for isotropic reorientational motion. The rotational diffusion coefficients are (from top to bottom): $3 * 10^8$ s^{-1}, 10^8 s^{-1}, $3 * 10^7$ s^{-1}, 10^7 s^{-1}, and $3 * 10^5$ s^{-1}. Spectra simulation parameters are: $g_{xx} = 2.0090$, $g_{yy} = 2.0065$, $g_{zz} = 2.0025$, $A_{xx} = A_{yy} = 5$ G, and $A_{zz} = 34.1$ G, $T_2^{-1} = 2.5$ G. The dashed lines shows simulated spectra using Freed's program (Freed, 1976).

To test our approach we compare the stochastic dynamic EPR spectra with fitted spectra calculated by the slow motional EPR spectra simulation program of Freed (Schneider and Freed, 1989). This program is known to give excellent fits to accurate experimental spectra of isotropically diffusing radicals in a wide correlation time range. The variable fitting parameters were the rotational diffusion coefficient D and the additional line width parameter T_2. The comparison in Fig. 6 reveals good agreement of the spectral shapes and splittings calculated with both programs within the total correlation time range shown. The values of the fitted diffusion coefficients D_{calc} agree well with those used to calculate the respective trajectory.

The phase memory time TM

The method of stochastic dynamics EPR simulations provides the calculation of the phase memory time *TM*. The phase memory time represents the contribution of irreversible mechanisms to the transversal relaxation time T_2. The line shape of the central field line was calculated for a single initial orientation corresponding to the absorption line maximum. In the range of the reorientation correlation time τ between 0.5 and 1700 ns, the peak to peak widths of the first derivative absorption line generated by 300 trajectories were determined. The results are shown in Fig. 7. The behavior of the simulated *TM* values agrees well with values determined from CW and ESE measurements on PD-Tempone (Stillman et al., 1980).

All simulations presented here were performed on a Pentium 90 personal computer. Typical computation times are 40 min for 80 orientation trajectories and additional 60 min for the calculation of a spectrum.

The spin-labeled polyleucine trimer

From the angle population densities (Fig. 5) smooth potential energy surfaces are calculated as described in Methods. A superposition of two Gaussian functions (Eq. 7) is found to be sufficient to guarantee that the succeeding single particle stochastic dynamic simulations show a similar angle population density behavior as the respective densities given in Fig. 5. EPR spectra are simulated from 200 trajectories of these single particle stochastic dynamics calculations with 100 different sine β weighted orientations of the polypeptide. This yields a total of 20,000 magnetization trajectories. In all three cases a diffusion coefficient of $D =$

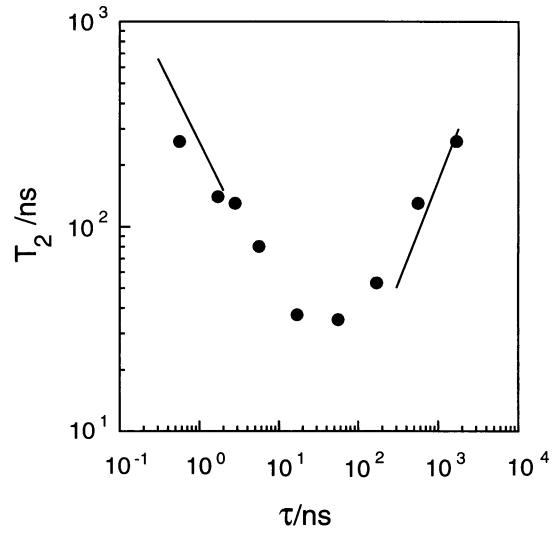

FIGURE 7 Simulated phase memory times TM for isotropic Brownian reorientational diffusion as a function of the reorientation correlation time τ determined for the center line. The lines show the experimental TM values that were determined by means of electron spin echo techniques for a nitroxide radical solved in glycerol (Stillman et al., 1984).

0.05 ns^{-1} corresponding to an isotropic rotational correlation time of 3 ns is used to account for the frictional effect of side chains and solvent molecules. The other parameters chosen are: $g_{xx} = 2.0090$, $g_{yy} = 2.0065$, $g_{zz} = 2.0025$, $A_{xx} = A_{yy} = 5$ G, $A_{zz} = 34.1$ G. The resulting first derivative EPR spectra are shown in Fig. 8 *a*. The increasing interaction with the tertiary structure of spin label side chain 1 to 3 is reflected in the observed increase of the spectral splitting.

It is of interest to compare these simulated spectra with experimental spectra on protein bound spin labels determined for comparable tertiary structure of the spin label environment. Recent EPR experiments with the R1 side chain on the D-helix of bacteriorhodopsin show an increase in immobilization through the sequence from residue 105 to 127 (Altenbach et al., 1994). The character of the tertiary interaction of sites 105 to 127 changes in a manner similar to that for spin labels 1 to 3 in our study. For comparison, the spectra of the spin-labeled bacteriorhodopsin with the spin label bound to 105, 109, 124, and 127 are shown in Fig. 8 *b*, with a projection of the CDE-helices at the level of the spin label (Fig. 8 *c*). The atomic data were those of the native protein taken from the Brookhaven Protein Data Bank (Henderson et al., 1990). The tertiary structure in the environment of 105 and 109 is similar to that of spin label 1, and the spin label side chain does not interact with neighboring helices. For sites 124 and 127 the C_β-C_α bond is oriented toward to an adjacent helix. Thus, restrictions for dihedral angle fluctuations are expected in these cases, similar to spin labels 2 and 3 in our model system. A comparison demonstrates that the experimental spectra of the spin labels bound to these sites are similar to the simulated spectra of spin labels 2 and 3.

DISCUSSION

To understand the interaction mechanisms that influence the spin label side-chain motion in a protein, first a stochastic dynamics simulation of a spin label attached to an isolated, fixed cysteine has been performed at 300 K. Steric interaction and torsion barriers lead to anisotropic reorientation of the attached spin label. The biphasic correlation function results in characteristic time constants of 6 and 100 ps. The fast decay is similar to the reorientation correlation time of a nitroxide diffusing freely in solution. The friction coefficient used amounts to one third of the viscosity of water at 295 K. Thus, we would expect the upper limit of the reorientation correlation time of an R1 side chain to be close to 300 ps in aqueous solution, if interaction with secondary or tertiary structure are not considered.

The stochastic dynamics simulations of the spin-labeled α-helix (spin label 1, cf. Fig. 1) reveal that the motion of the spin label side chain depends significantly on the interaction with the backbone. The trajectory displays two major types of fluctuations. On a short time scale (1 ps), angle fluctuations with rms amplitudes from 14° to 23° are found that represent oscillations within discrete potential minima. On a longer time scale, jumps between these potential valleys occur with orientation changes of large amplitudes ($\geq$30°). For the reorientation jumps at 300 K a correlation time of ~500 ps is estimated. A similar behavior has been reported for other systems: the reorientation of a methemoglobin bound spin label (Steinhoff and Karim, 1993) and the interproton dihedral angle fluctuations of side chains in lysozyme (Dobson and Karplus, 1986). The correlation time should approach 1.5 ns for the helix-bound nitroxide in an aqueous environment, if proportionality holds between reorientation correlation time and viscosity. However, because of the lack of water molecules in the simulations, we have to be careful in comparing the values of the correlation time determined above with experimental data. The attractive van der Waals interaction between the helix and the spin label side chain may be altered resulting in an overestimation of the motional restriction. In contrast, the hydrophobic interaction would increase the attraction between backbone and the hydrophobic spin label side chain. In

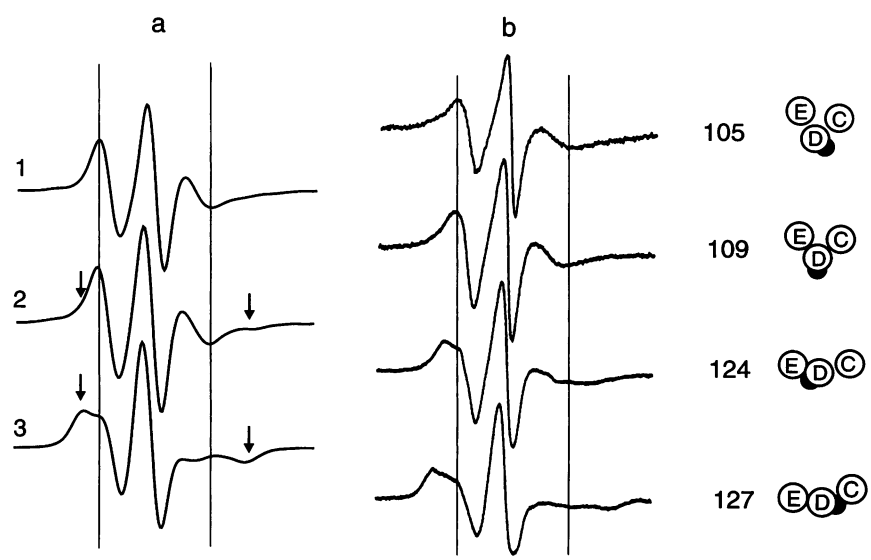

FIGURE 8 Comparison of experimental EPR spectra with EPR spectra simulated from Brownian dynamics trajectories. (*a*) Simulated EPR spectra. The effective potentials were calculated from the angle population densities shown in Fig. 5. The rotation diffusion coefficient is set to 0.05 ns^{-1}. The *g*- and *A*-tensor values are given in the legend of Fig. 6. The spectra have been convoluted with a Gaussian of 2.5 G width to account for inhomogeneous broadening mechanisms. (*b*) Experimental EPR spectra for spin-labeled bacteriorhodopsin D-helix mutants and slices through the C-D-E helical region of bacteriorhodopsin. Each slice is taken in a plane containing the indicated residue. The dot identifies the position of the β carbon atom of the spin label side chain.

addition, experimental studies demonstrated, that the dynamics of water molecules on the surface of a protein is significantly slowed down when compared to that of free water. This leads to an increase of the viscosity of the spin label side-chain environment (Steinhoff et al., 1993). These mechanisms, the reduction of van der Waals attraction and the hydrophobic interaction or the increased viscosity, have opposite effects on the reorientation dynamics of the spin label side chain and may partly cancel. The results of site-directed spin labeling studies of colicin E1 (Todd et al., 1989) and of β-lactamase (Todd and Millhauser, 1991) indicate that the reorientation of the spin label side chain on the surface of an α-helix in aqueous solution is of the order of 1.3–3 ns, which shows that the results of our simulations agree strikingly well with the experiment.

Because of the significant interaction of the spin label side chain with the helix backbone, local dynamics of the secondary structure should increase the overall reorientational dynamics of the spin label side chain. In fact, this is observed in experimental studies. Millhauser and co-workers report a position-dependent dynamics of spin labels attached to alanine-based helical peptides (Miick et al., 1993): enhanced dynamics was found at the peptide termini. They report also significant changes of the spin label side-chain motion during the α-helix-random coil transition (Miick et al., 1991; Todd and Millhauser, 1991).

To study the angle distribution of the reorientational motion of the R1 side chain, high temperature stochastic dynamics simulations have been performed to guarantee that the whole accessible angle space is covered within the simulation time. The anisotropic behavior of the reorientational motion of the trimer bound spin labels is revealed by the angle population density plots calculated from these simulations (Fig. 5). The interaction energy for reorientational motion of spin label 1 consists of torsion terms and a relatively small number of nonbonded interactions between the moving atoms of the nitroxide side chain and the stationary atoms of the backbone. This interaction shows probability distribution maps with multiple extremes in various regions of the side-chain orientation angles and thus leaves wide regions of low energy. The overall angle distribution is nearly isotropic. This is still true for the spin label in position 2, where the isotropic part of the angle distribution is superimposed by two broad population maxima. The high flexibility of the nitroxide side chain is mainly due to fluctuations of the dihedrals $\Psi_{C3\text{-}C}$ and $\Psi_{C\text{-}S}$; nonbonded contacts of the sulfurs with backbone atoms seem to prevent large fluctuations of $\Psi_{S\text{-}C\beta}$ and $\Psi_{C\beta\text{-}C\alpha}$ (cf. Table 1). As soon as the number of nonbonded interaction is increased, as for the spin label attached to position 3, the angle population map shows sharp, well-defined maxima. In this case, the two resulting energy minima are separated by a 180° rotation as a consequence of the structural symmetry of the nitroxide ring. This behavior is most likely true for ring structures in the interior of proteins as reported for the eight aromatics within pancreatic trypsin inhibitor (Gelin and Karplus, 1979). The reorientation probability for these 180° turns is low as can be judged from the trajectory (Fig. 4 *d*), because a number of correlated rotations around the C_3-C, C-S, and C_β-C_α bonds are necessary (cf. Table 1).

We have shown that a Hamiltonian can be found that allows EPR spectra to be calculated from stochastic dynamics simulation trajectories of the considered spin labels. Extending the algorithm described by Robinson et al. (1992), the pseudosecular terms are included within our approach. The averaging of these terms due to molecular motion is empirically found to be governed by the correlation function of the reorientation of the nitroxide z axes. A comparison of simulated EPR spectra with calculations using Freed's program (Freed, 1976; Schneider and Freed, 1989) for isotropic Brownian diffusion shows that the chosen approach yields EPR spectra with correct splittings, line shapes, and transverse relaxation times (cf. Figs. 6 and 7). Thus, the means are now available to perform quantitative comparisons of experimental EPR spectra and spectra and those simulated from stochastic-dynamic methods.

Trajectories have been calculated from numerical solutions of the Langevin equation with free energy surfaces taken from the population densities shown in Fig. 5. The EPR spectra calculated from these trajectories clearly reflect the different degrees of immobilization for the three cases studied (Fig. 8 *a*). In all three cases the simulations are performed with a diffusion coefficient set to a corresponding isotropic correlation time of 3 ns. From the discussion of the correlation times found for our 300 K simulations and from experimental studies this seem to be a proper value. The splitting and the line shapes of the simulated spectra are in good agreement with experimental spectra of the R1 side chain on the D-helix of bacteriorhodopsin in comparable secondary and tertiary environments. The increase of motional restrictions due to tertiary interaction are visible in the appearance of outer peaks in the low field and high field extremes of both, the simulated and the experimental spectra.

The study of the orientation of helix D with respect to the protein is of special interest because the coordinates of this helix are known with only limited resolution. So far, our results show qualitative agreement of the spin label binding site structures of the D-helix taken from the protein data bank with those of the model trimer. One of the next steps will be to perform stochastic dynamics simulations of attached spin labels on the basis of the available atomic data of bacteriorhodopsin. Successive variation of the starting coordinate set and comparison of the simulated EPR spectra with experiments should lead to a refinement of the D-helix coordinate set and to proposals of loop structures.

CONCLUSION

EPR spectra simulations based on stochastic dynamics simulations of peptide-bound spin labels are feasible within reasonable expense of computation time. The results indicate that the immobilization seen in room temperature EPR

spectra of protein bound MTS spin labels can be explained by the interaction of the nitroxide group side chain with atoms of neighboring helices or loops. The spectral shape is characteristic for the secondary and tertiary structure and its dynamics in the spin label binding site environment.

Site-directed mutagenesis has made it possible to spin label nearly every desired site in a protein. With a whole set of spin-labeled proteins and the respective molecular dynamic simulations a structural refinement of low resolution diffraction data, for example, should be possible. However, one of the greatest strengths of the EPR spin labeling method is its time resolution. Using the site directed spin-labeling method, structural changes in bR during the photocycle could be detected (Steinhoff et al., 1994, 1995). The application of EPR spectra simulations to this subject opens the door to characterize structural changes with atomic resolution.

We gratefully acknowledge a grant by the Max Kade Foundation (H.-J.S.), National Institutes of Health grant EY05216 and the Jules Stein Professor endowment (W.L.H.). Part of this work was funded by the Deutsche Forschungsgemeinschaft (Ste 640/2-1-685/94) to H.-J.S.

REFERENCES

Altenbach, C., T. Marti, H. G. Khorana, and W. L. Hubbell. 1990. Transmembrane protein structure: spin labeling of bacteriorhodopsin mutants. *Science.* 248:1088–1092.

Altenbach, C., D. Greenhalgh, H. G. Khorana, and W. L. Hubbell. 1994. A collision gradient method to determine the immersion depth of nitroxides in lipid bilayers: application to spin-labeled mutants of bacteriorhodopsin. *Proc. Natl. Acad. Sci. USA.* 91:1667–1671.

Altenbach, C., H.-J. Steinhoff, D. A. Greenhalgh, H. G. Khorana, and W. L. Hubbell. 1994. Factors that determine the EPR spectra of nitroxide side-chains in spin labeled proteins and analysis by molecular dynamics simulation. *Biophys. J.* 65a:40.

L. J. Berliner, Spin Labeling I, Theory, and Application. Academic Press Inc., New York, 1976.

L. J. Berliner, Spin Labeling II, Theory, and Application. Academic Press Inc., New York, 1979.

Berliner, L. J., and J. Reuben. 1989. Biological Magnetic Resonance 8, Spin Labeling. Plenum Press, New York.

Brooks, C. L. III. 1995. Methodological advances in molecular dynamics simulations of biological systems. *Curr. Opin. Struct. Biol.* 5:211–215.

Freed, J. H. 1976. Theory of slow tumbling ESR spectra for nitroxides. *In* Spin Labeling Theory and Applications. L. J. Berliner, editor. Academic Press, New York. 53–132.

Gelin, B. R., and M. Karplus. 1979. Side chain torsional potentials: effects of dipeptide, protein and solvent environment. *Biochemistry.* 18: 1256–1268.

Ge, M., and J. Freed. 1993. An electron spin resonance study of interactions between gramicidin A′ and phosphatidylcholine bilayers. *Biophys. J.* 65:2106–2123.

Gunsteren, van, W. F., H. J. C. Berendsen, and J. A. C. Rullmann. 1981. Stochastic dynamics for molecules with constrains, Brownian dynamics of *n*-alkanes. *Mol. Phys.* 44:69–95.

Gunsteren, van, W. F., and H. J. C. Berendsen. 1982. Algorithms for brownian dynamics. *Mol. Phys.* 45:637–647.

Henderson, R., J. M. Baldwin, T. A. Ceska, F. Zemlin, E. Beckmann, and K. H. Downing. 1990. Model for the structure of bacteriorhodopsin based on high-resolution electron cryo-microscopy. *J. Mol. Biol.* 213: 899–929.

Hubbell, W. L., and C. Altenbach. 1994. Investigation of structure and dynamics in membrane proteins using site-directed spin labeling. Current opinions in struct. *Biology.* 4:566–573.

Libertini, L. J., and O. H. Griffith. 1970. Orientation dependence of the electron spin resonance spectrum of di-*t*-butyl nitroxide. *J. Chem. Phys.* 53:1359–1367.

Jolicoeur, C., and H. L. Friedman. 1971. Effects of hydrophobic interactions on dynamics in aqueous solutions studied by EPR. *Ber. Bunsenges. Phys. Chem.* 75:248–257.

Miick, S. M., A. P. Todd, and G. L. Millhauser. 1991. Position-dependent local motions in spin-labeled analogues of a short α-helical peptide determined by electron spin resonance. *Biochemistry.* 30:9498–9503.

Miick, S. M., K. M. Casteel, and G. L. Millhauser. 1993. Experimental molecular dynamics of an alanine-based helical peptide determined by spin label electron spin resonance. *Biochemistry.* 32:8014–8021.

Robinson, B. H., L. J. Slutsky, and F. P. Auteri. 1992. Direct simulation of continuous wave electron paramagnetic resonance spectra from Brownian dynamics trajectories. *J. Chem. Phys.* 96:2609–2616.

Schneider, D. J., and J. H. Freed. 1989. Calculating slow motional magnetic resonance spectra: a users guide. *In* Biological Magnetic Resonance 8, Spin Labeling. L. J. Berliner and J. Reuben, editors. Plenum Press, New York. 1–76.

Steinhoff, H.-J. 1988. A simple method for determination of rotational correlation times and separation of rotational and polarity effects from EPR spectra of spin-labeled biomolecules in a wide correlation time range. *J. Biochem. Biophys. Methods.* 17:237–248.

Steinhoff, H.-J., K. Lieutenant, and J. Schlitter. 1989. Residual motion of hemoglobin-bound spin labels as a probe for protein dynamics. *Z. Naturforsch.* 44c:280–288.

Steinhoff, H.-J. 1990. Residual motion of hemoglobin-bound spin labels and protein dynamics: viscosity dependence of the rotational correlation times. *Eur. Biophys. J.* 18:57–62.

Steinhoff, H.-J., and C. Karim. 1993. Protein dynamics and EPR-spectroskopy: comparison of molecular dynamic simulations with experiment. *Ber. Bunsenges. Phys. Chem.* 97:163–171.

Steinhoff, H.-J., B. Kramm, G. Hess, C. Owerdieck, and A. Redhardt. 1993. Rotational and translational water diffusion in the hemoglobin hydration shell: dielectric and proton nuclear relaxation measurements. *Biophys. J.* 65:1486–1495.

Steinhoff, H.-J., R. Mollaaghababa, C. Altenbach, K. Hideg, M. Krebs, H. G. Khorana, and W. L. Hubbell. 1994. Time-resolved detection of structural changes during the photocycle of spin-labeled bacteriorhodopsin. *Science.* 266:105–107.

Steinhoff, H.-J., R. Mollaaghababa, C. Altenbach, H. G. Khorana, and W. L. Hubbell. 1995. Site directed spin labeling studies of structure and dynamics in bacteriorhodopsin. *Biophys. Chem.* 56:89–94.

Stillman, A. E., L. J. Schwartz, and J. H. Freed. 1980. Direct determination of rotational correlation time by electron-spin echoes. *J. Chem. Phys.* 73:3502–3503.

Todd, A. P., J. Cong, F. Levinthal, C. Levinthal, and W. L. Hubbell. 1989. Site-directed mutagenesis of colicin E1 provides specific attachment sites for spin labels whose spectra are sensitive to local conformation. *Proteins.* 6:294–305.

Todd, A. P., and G. L. Millhauser. 1991. ESR spectra reflect local and global mobility in a short spin-labeled peptide throughout the α-helix-coil transition. *Biochemistry.* 30:5515–5523.

Van, S. P., G. B. Birrell, and O. H. Griffith. 1974. Rapid anisotropic motion of spin labels. Models for motion averaging of the ESR parameters. *J. Magn. Reson.* 15:444–459.

Wolynes, P. G., and J. M. Deutch. 1977. Dynamical orientation correlations in solution. *J. Chem. Phys.* 67:733–741.